Production of InSAR data and secular line-of-sight velocities of Southern California for the Community Geodetic Model: summary

Abstract

The objective of the project is to produce InSAR data and estimate average deformation velocities in support of the SCEC Community Geodetic Model (CGM) project. We process SAR interferograms using archival data acquired by the European ERS and Envisat missions, spanning the period 1992–2011, from seven descending tracks covering the southern California region. This processing effort aims to supply standard interferogram products, produced according to a 'best practice' specification, developed at past CGM workshops, to be used to test time series inversion methods and to ultimately produce a combined GPS/InSAR consensus deformation product. To facilitate this, interferogram data produced under this project will be archived in the InSAR Product Archive at UNAVCO (https://winsar.unavco.org/insar/) for use by other CGM participants and in future CGM products. We apply the small baseline subset method to our processed interferograms to estimate average line-of-sight (LOS) velocities for each track. We find that the majority of the deformation captured by our InSAR data is consistent with plate-boundary parallel shear at rates of 3–4 cm/yr (equivalent to 1.0–1.3 cm/yr in LOS velocity), in a zone including the San Andreas and San Jacinto faults.

Intellectual merit

The project aligns well with and advances SCEC5 science goals. Development of community models is a SCEC5 Thematic Area, and our project directly addresses the Tectonic Geodesy research priority: "Produce a consensus secular velocity InSAR product using the full archive of SAR data (ERS, Envisat, ALOS-1) for the SCEC region." (2017 Science Collaboration Plan, pg 19). The data products (interferograms and line-of-sight velocity maps) produced within the project will be used to answer what the fault loading rates in southern California are, and to constrain locations and amounts of off-fault deformation (both are SCEC5 'Basic Questions of Earthquake Science').

Broader impacts

SCEC Community Models are inherently infrastructure projects, creating data products that will be used broadly, and for multiple purposes. This project explicitly is targeted to produce data in support of the Community Geodetic Model (CGM) project. Within SCEC and the earthquake science community, such products may be used in the construction of earthquake hazard models, which themselves have a much broader potential reach than just the earthquake science community – to industry, local government and society as a whole. Deformation datasets like the CGM can also be potentially useful for monitoring other processes, such as groundwater withdrawal/change, landsliding, subsidence and changes to vulnerable infrastructure. Our results are thus of potential use to many other groups.

Production of InSAR data and secular line-of-sight velocities of Southern California for the Community Geodetic Model: technical report

Gareth Funning (University of California, Riverside)
Zhen Liu (Jet Propulsion Laboratory)

Introduction and background

The SCEC Community Geodetic Model (CGM) is an ongoing project within SCEC5 with the goal of producing consensus geodetic deformation products for southern California. These products, including secular velocities and deformation time series compiled from campaign and continuous GPS measurements, and from InSAR data from multiple platforms will be combined into a combined, consensus product honoring both data types. This 'geodetic model' will be used in multiple research areas within SCEC, e.g. providing constraints on fault loading rates, aseismic creep and off-fault deformation for earthquake hazard models.

Since 2013, the Tectonic Geodesy group within SCEC has led efforts to identify best practices for producing InSAR deformation time series and secular velocity maps. These have included several comparative tests of different processing strategies, and a series of in-person and virtual workshops. At a CGM workshop in Pomona in January 2016, the InSAR contributors of the CGM group used these experiences to compile a set of best practices for interferogram processing and post-processing. We use these here to produce preliminary InSAR products for the CGM project: a comprehensive set of SAR interferograms from the ERS and Envisat missions covering the SCEC region, which will then be used to estimate a secular line-of-sight velocity product using the mature SBAS (Small BAseline Subset) method. We aim to share these interferograms and velocity products with the CGM group and the wider community via a publicly hosted archive at UNAVCO (the interferograms) and, when available, the new CGM website (the velocity products).

SAR data selection

We select data from seven descending ERS/Envisat beam I2 tracks (Figure 1). These cover the majority of the southern California plate boundary zone, from the creeping segment of the San Andreas fault in the northwest, to the Salton Trough in the southwest. The majority of these data are held in the WInSAR and GeoEarthScope archives maintained by UNAVCO; we download them as raw (unfocused) data.

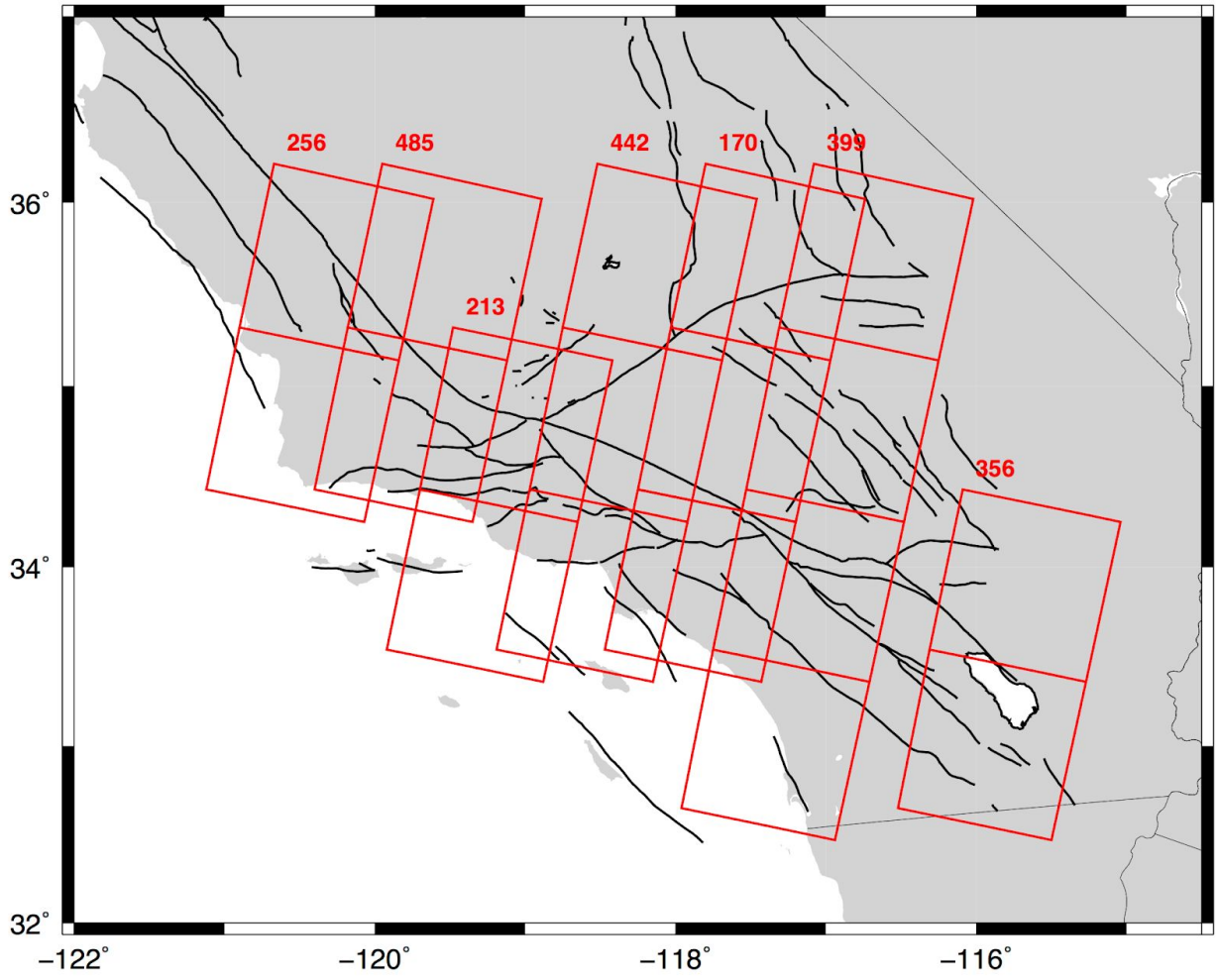

Figure 1: SAR data coverage for this project. Seven descending tracks of the ERS and Envisat missions are shown (red), labeled by their track numbers.

Processing methodology

We process the ERS and Envisat data using the JPL/Caltech ROI_PAC software (Rosen et al., 2002) according to the best practices identified by the CGM group:

- **Interferometric pair selection:** We select pairs of SAR images that meet defined thresholds for perpendicular baselines (< 200 m) and time spans (< 2 years) for processing as interferograms. Some possible interferometric pairs using data from the ERS-2 satellite, acquired after that satellite's gyroscope systems failed in late 2000, are ultimately excluded from our dataset on the basis of incompatible Doppler centroids. In order to enhance connectivity in our interferogram 'networks' we additionally add some

pairs with longer time span and near-zero perpendicular baselines. In practice, we obtain 250–350 useable interferometric pairs on each track.

- **Orbit corrections:** We use Delft precise orbits (e.g. Scharoo and Visser, 1998) to correct for orbital phase. We do not re-estimate the orbital baseline to correct for long-wavelength ramps, as recent studies have shown that other long-wavelength errors, such as local oscillator drift and static troposphere, can erroneously map into that correction (e.g. Fattahi and Amelung, 2014).
- **Topographic corrections:** We use a downsampled, 2 arcsecond SRTM DEM (e.g. Farr et al., 2007) to correct for topographic artifacts.
- **Filtering:** To improve signal-to-noise in our interferograms, we first multilook (spatially average) our data, taking 4 range looks and 20 azimuth looks. Next, to enhance short-to-medium wavelength signal we additionally apply an adaptive power spectrum filter (e.g. Goldstein and Werner, 1998) with a filter exponent of 0.5.
- **Local oscillator drift:** To remove the temporally correlated range ramp error due to drift of the Envisat ASAR sensor, we apply the empirical relationship of Marinkovic and Larsen (2015) as a correction to our Envisat interferograms.
- **Unwrapping:** We use the minimum cost flow unwrapper from the snaphu package (Chen and Zebker, 2002) to unwrap our interferograms. Pixels with interferometric correlation below 0.25 are masked out during this process.

Post-processing and archiving

We use a variant of the small baseline subset (SBAS) algorithm (e.g. Berardino et al., 2002) to solve for the best average line-of-sight (LOS) velocities for each coherent pixel on each track. We show some examples of the LOS velocity maps produced in Figure 2. In general, the LOS velocity change across the major fault structures of the plate boundary zone (the San Andreas fault in the NW of our area of interest, and the San Andreas and San Jacinto faults in the SE) is in the range 1.0–1.3 cm/yr; given the descending track viewing geometry, this translates to plate boundary-parallel horizontal deformation rates in the range 3–4 cm/yr, in keeping with estimates of plate boundary deformation rates from geology and GPS (e.g. DeMets et al., 2010). Superimposed on the plate boundary deformation are multiple small-spatial wavelength, large amplitude deformation signals, consistent with locations of major groundwater basins (e.g. the Santa Ana aquifer; Argus et al., 2005) or areas of hydrocarbon production (e.g. the Lost Hills oil field; Fielding et al., 1998). We plan to share these datasets through the CGM website, when it is updated.

We are also currently preparing to archive the interferogram data produced under this project for community and CGM use. We plan to convert the data to HDF5 format for archiving in the InSAR Product Archive at UNAVCO (https://winsar.unavco.org/insar/) where the data will be citeable, via digital object identifiers (DOIs).

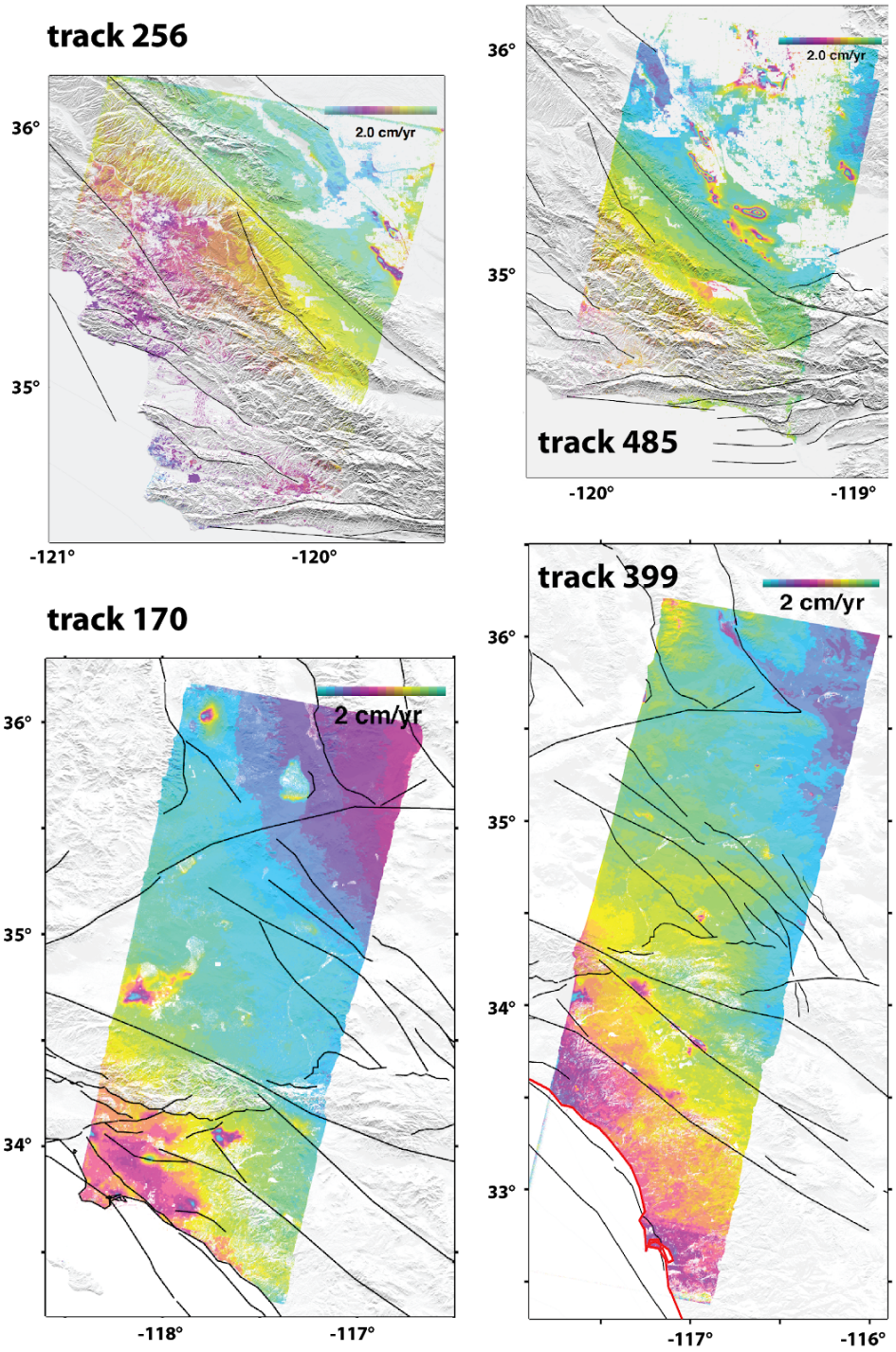

Figure 2: Examples of InSAR line-of-sight (LOS) velocity maps for four of the tracks processed (see Figure 1 for locations). Velocities are wrapped at a 2 cm/yr interval. In each case, deformation across the main plate boundary fault structures is in the range 1.0–1.3 cm/yr in LOS velocity; locally, larger amplitude velocity features (small 'blobs') are collocated with groundwater basins and oil production fields.

References

Argus, D. F., M. B. Heflin, G. Peltzer, F. Crampé, and F. H. Webb (2005), Interseismic strain accumulation and anthropogenic motion in metropolitan Los Angeles, J. Geophys. Res., 110, B04401, doi: 10.1029/2003JB002934.

Berardino, P., G. Fornaro, R. Lanari and E. Sansosti, 2002, A New Algorithm for Surface Deformation Monitoring Based on Small Baseline Differential SAR Interferograms, IEEE Trans. Geosci. Rem. Sens., 40, 2375–2383, doi:10.1109/TGRS.2002.803792.

Chen, C. W. and H. A. Zebker, 2002, Phase unwrapping for large SAR interferograms: Statistical segmentation and generalized network models, IEEE Trans. Geosci. Rem. Sens., 40, 1709-1719.

DeMets, C., R. G. Gordon, and D. F. Argus, 2010, Geologically current plate motions. Geophys. J. Int., 181: 1-80. doi:10.1111/j.1365-246X.2009.04491.x

Farr, T. G., P. A. Rosen, E. Caro, R. Crippen, R. Duren, S. Hensley, M. Kobrick, M. Paller, E. Rodriguez, L. Roth, D. Seal, S. Shaffer, J. Shimada, J. Umland, M. Werner, M. Oskin, D. Burbank and D. Alsdorf, 2007, The Shuttle Radar Topography Mission, Rev. Geophys., 45, RG2004, doi:10.1029/2005RG000183.

Fattahi, H. and F. Amelung, 2014, InSAR uncertainty due to orbital errors, Geophys. J. Int., 199, 549–560, doi:10.1093/gji/ggu276.

Fielding, E. J., R. G. Blom, and R. M. Goldstein, 1998, Rapid subsidence over oil fields measured by SAR interferometry, Geophys. Res. Lett., 25, 3215-3218.

Goldstein, R. M. and C. L. Werner, 1998, Radar interferogram filtering for geophysical applications, Geophys. Res. Lett., 25, 4035-4038.

Marinkovic, P. and Y. Larsen, 2015, On resolving the Local Oscillator drift induced phase ramps in ASAR and ERS1/2 interferometric data – the final solution (abstract), European Space Agency FRINGE 2015, Frascati, Italy.

Scharroo, R. and P. Visser, 1998, Precise orbit determination and gravity field improvement for the ERS satellites, J. Geophys. Res, 103 (C4), 8113–8127.